Journal of Experimental Botany
https://doi.org/10.1093/jxb/erac421 Advance Access Publication 27 October, 2022

RESEARCH PAPER

Metabolic link between auxin production and specialized metabolites in *Sorghum bicolor*

Veronica C. Perez[1,†], Ru Dai[2,†], Breanna Tomiczek[3], Jorrel Mendoza[4], Emily S.A. Wolf[1], Alexander Grenning[3], Wilfred Vermerris[1,5,6,7], Anna K. Block[4] and Jeongim Kim[1,2,*]

[1] Plant Molecular and Cellular Biology Program, University of Florida, Gainesville, FL 32611, USA
[2] Horticultural Sciences Department, University of Florida, Gainesville, FL 32611, USA
[3] Department of Chemistry, University of Florida, Gainesville, FL 32611, USA
[4] Chemistry Research Unit, Center for Medical, Agricultural and Veterinary Entomology, U.S. Department of Agriculture-Agricultural Research Service, Gainesville, FL 32608, USA
[5] Department of Microbiology & Cell Science, Gainesville, FL 32611, USA
[6] UF Genetics Institute, University of Florida, Gainesville, FL 32611, USA
[7] Florida Center for Renewable Chemicals and Fuels, University of Florida, Gainesville, FL 32611, USA

† These authors contributed equally to this work.
* Correspondence: jkim6@ufl.edu

Received 8 April 2022; Editorial decision 10 October 2022; Accepted 18 October 2022

Editor: Ros Gleadow, Monash University, Australia

Abstract

Aldoximes are amino acid derivatives that serve as intermediates for numerous specialized metabolites including cyanogenic glycosides, glucosinolates, and auxins. Aldoxime formation is mainly catalyzed by cytochrome P450 monooxygenases of the 79 family (CYP79s) that can have broad or narrow substrate specificity. Except for SbCYP79A1, aldoxime biosynthetic enzymes in the cereal sorghum (*Sorghum bicolor*) have not been characterized. This study identified nine CYP79-encoding genes in the genome of sorghum. A phylogenetic analysis of CYP79 showed that SbCYP79A61 formed a subclade with maize ZmCYP79A61, previously characterized to be involved in aldoxime biosynthesis. Functional characterization of this sorghum enzyme using transient expression in *Nicotiana benthamiana* and stable overexpression in *Arabidopsis thaliana* revealed that SbCYP79A61 catalyzes the production of phenylacetaldoxime (PAOx) from phenylalanine but, unlike the maize enzyme, displays no detectable activity against tryptophan. Additionally, targeted metabolite analysis after stable isotope feeding assays revealed that PAOx can serve as a precursor of phenylacetic acid (PAA) in sorghum and identified benzyl cyanide as an intermediate of PAOx-derived PAA biosynthesis in both sorghum and maize. Taken together, our results demonstrate that SbCYP79A61 produces PAOx in sorghum and may serve in the biosynthesis of other nitrogen-containing phenylalanine-derived metabolites involved in mediating biotic and abiotic stresses.

Keywords: Aldoximes, auxin biosynthesis, benzyl cyanide, PAA, sorghum.

Abbreviations: PAA, phenylacetic acid; PAOx, phenylacetaldoxime.

Introduction

Plants produce a wide variety of specialized metabolites that are structurally and functionally diverse and that play crucial roles in plant stress adaptation. Aldoximes are nitrogen-containing imines derived from amino acids that serve as precursors of various specialized metabolites including cyanogenic glycosides and glucosinolates, which function in plant defense against herbivores and pathogens (Sørensen *et al.*, 2018). For example, the tyrosine-derived aldoxime 4-hydroxyphenylacetaldoxime is a precursor of dhurrin in sorghum (*Sorghum bicolor*) (Koch *et al.*, 1995; Sibbesen *et al.*, 1995), triglochinin in *Triglochin maritima* (Nielsen and Møller, 1999), taxiphyllin in *Taxus baccata* (Luck *et al.*, 2017), and tyrosol in *Sinapis alba* (Kindl and Schiefer, 1971). The phenylalanine-derived aldoxime phenylacetaldoxime (PAOx) is a precursor of the cyanogenic glycosides amygdalin and prunasin in species such as almond (*Prunus dulcis*), apricot (*Prunus meme*), and apples (*Malus domestica*) (Yamaguchi *et al.*, 2014; Bolarinwa *et al.*, 2015; Hansen *et al.*, 2018; Thodberg *et al.*, 2018). Aliphatic aldoximes also participate in cyanogenic glycoside biosynthesis, serving as intermediates in the conversion of valine to linamarin in flax (*Linum usitatissimum*) and cassava (*Manihot esculenta*) (Tapper *et al.*, 1967; Andersen *et al.*, 2000), as well as in the conversion of isoleucine to lotaustralin in cassava and lima bean (*Phaseolus lunatus*) (Andersen *et al.*, 2000; Lai *et al.*, 2020). In Brassicales, aldoximes are precursors of glucosinolates (Underhill, 1967; Bak *et al.*, 1998; Halkier and Gershenzon, 2006; Blažević *et al.*, 2020) and the phytoalexin camalexin (Glawischnig *et al.*, 2004; Glawischnig, 2007). Various volatiles including 2-phenylethanol (Dhandapani *et al.*, 2019), (2-nitroethyl)benzene (Yamaguchi *et al.*, 2021), and nitriles are generated from aldoximes and contribute to the herbivore-induced volatile blend of many species (Irmisch et al., 2013, 2014; McCormick *et al.*, 2014; Luck *et al.*, 2016; Yamaguchi *et al.*, 2016).

Aldoxime production from regular or chain-elongated amino acids is catalyzed mainly by cytochrome P450 enzymes belonging to family 79 (CYP79). For example, CYP79A2 from Arabidopsis and CYP79D73 from *Plumeria rubra* catalyze PAOx production from phenylalanine (Dhandapani *et al.*, 2019; Wittstock and Halkier, 2000), CYP79B2 and CYP79B3 from Arabidopsis catalyze indole-3-acetaldoxime (IAOx) production from tryptophan (Mikkelsen *et al.*, 2000; Zhao, 2002), and CYP79F1 and CYP79F2 act upon chain-elongated methionine (Chen *et al.*, 2003) in Arabidopsis to produce aliphatic aldoximes that are precursors of aliphatic glucosinolates (Harun *et al.*, 2020). Other CYP79 enzymes have greater promiscuity, such as poplar (*Populus trichocarpa*) CYP79D6 and CYP79D7, which can generate aldoximes from tryptophan, phenylalanine, isoleucine, leucine, and tyrosine (Irmisch *et al.*, 2013). Recently, heterologous expression analyses demonstrated that the Arabidopsis enzymes CYP79C1 and CYP79C2 have promiscuous aldoxime production activity, with CYP79C2 acting mainly upon leucine and phenylalanine, but with minor activity towards isoleucine, tryptophan, and tyrosine, whereas CYP79C1 acts upon leucine, isoleucine, phenylalanine, and valine (Wang *et al.*, 2020). CYP79 enzymes are widely distributed in both monocots and dicots, and have been identified in some gymnosperms (Sibbesen *et al.*, 1995; Nielsen and Møller, 2000; Irmisch et al., 2013, 2015; Yamaguchi et al., 2014, 2021; Luck et al., 2016, 2017; Hansen *et al.*, 2018; Sørensen *et al.*, 2018; Thodberg *et al.*, 2018; Dhandapani *et al.*, 2019; Lai *et al.*, 2020). There is also evidence for other flavin-containing monooxygenases (FMOs) that are capable of catalyzing aldoxime formation. Examples of such FMOs have been identified in fern and shown to be involved in PAOx formation (Thodberg *et al.*, 2020).

Aldoximes also play crucial roles in plant growth. Specifically, IAOx and PAOx are precursors of the two major auxins indole-3-acetic acid (IAA) and phenylacetic acid (PAA), respectively, in Brassicales and maize (*Zea mays*), although the molecular components of aldoxime-derived auxin biosynthesis remain to be elucidated (Zhao, 2002; Sugawara *et al.*, 2009; Aoi *et al.*, 2020; Perez *et al.*, 2021).

In maize, aldoxime-derived auxin biosynthesis is initiated by ZmCYP79A61, which is capable of catalyzing both IAOx and PAOx formation (Irmisch *et al.*, 2015). Sorghum (*Sorghum bicolor*) is a monocot that is closely related to maize (Schnable *et al.*, 2009) and cultivated globally for feed, food, fodder, and biofuel production (Paterson *et al.*, 2009). Sorghum is known to contain one aromatic aldoxime production enzyme SbCYP79A1, which acts upon tyrosine and is involved in the production of the defense compound dhurrin (Sibbesen *et al.*, 1995). Given the role of aldoximes in plant responses to biotic and abiotic stresses, and the growing interest in sorghum as a climate-resilient crop, a better understanding of aldoxime metabolism in sorghum will enable novel crop improvement strategies.

In this study, we mined the sorghum genome for *CYP79* homologs and identified nine candidate sequences, including one homolog closely related to the maize gene encoding ZmCYP79A61. Further characterization of this candidate (*SbCYP79A61*) via genetic studies and transient expression identified it as an enzyme capable of producing PAOx. Additionally, our stable isotope labeling assays identified that sorghum produces PAA from PAOx and that benzyl cyanide is an intermediate of PAOx-derived PAA production in both sorghum and maize.

Materials and methods

Plant material and growth conditions

Arabidopsis thaliana Col-0, maize B104, sorghum RTx430, and *Nicotiana benthamiana* were used as wild-type plants. After 3 d of cold treatment at 4 °C, Arabidopsis seeds were planted on soil and kept in a growth chamber at 21 °C with 16 h light/8 h dark. Sorghum and *N. benthamiana* seeds were planted directly on soil and kept at 25 °C with 16 h light/8 h dark. Maize seeds were imbibed with water for 1 h before being planted on

soil and kept at 25 °C with 16 h light/8 h dark. The Arabidopsis double mutant *cyp79b2 cyp79b3* (*b2b3*) and its genotyping method are described in Zhao (2002).

CYP79 sequence analysis and phylogenetic tree generation

BLASTp analysis (Altschul *et al.*, 1990) was performed with the *S. bicolor* v3.1.1 genome from Phytozome v12 (phytozome.jgi.doe.gov) using the protein sequence of maize ZmCYP79A61 as the query. Protein sequences of sorghum, maize, poplar, plumeria, and Arabidopsis CYP79 proteins were aligned using the MUSCLE algorithm (Edgar, 2004) (gap open, -2.9; gap extend, 0; hydrophobicity multiplier, 1.2; clustering method, UPGMA) implemented in Mega7 (Kumar *et al.*, 2018). Phylogenetic trees were constructed with Mega7 using a Neighbor–Joining algorithm (model/method, Poisson; substitution type, amino acid; rates among sites, uniform; gaps/missing data treatment, pairwise deletion deletion). A bootstrap resampling analysis with 1000 replicates was performed to evaluate tree topology.

Plasmid construction and transgenic plant growth

The *SbCYP79A61* coding sequence was retrieved from Phytozome v12. We confirmed the published sequence of *SbCYP79A61* by sequencing genomic DNA prepared from sorghum BTx623. Our sequencing data indicate that *SbCYP79A61* does not contain any introns. To generate *SbCYP79A61* overexpression constructs, the *SbCYP79A61* ORF was synthesized within the pUC57 vector (Genewiz, South Plainfield, NJ, USA). The synthesized entry vector was subsequently recombined with the destination vector pCC0995 (Weng *et al.*, 2010), in which expression of the ORF is under the control of the cauliflower mosaic virus (CaMV) 35S promoter to generate the *35S::SbCYP79A61* construct. The *35S::SbCYP79A61, 35S::ZmCYP79A61* (Perez *et al.*, 2021), and *35S::AtCYP79B2* (Zhang *et al.*, 2020) constructs were introduced into *Agrobacterium tumefaciens* (GV3101) following a method described by Zhang *et al.* (2020). All three constructs were used to transiently express CYP79 enzymes in *N. benthamiana*, described in the following section.

The *35S::SbCYP79A61*-containing *A. tumefaciens* GV3101 cells were additionally used to transform Arabidopsis wild type (Col-0) or *b2b3* mutants via a floral dipping method (Zhang *et al.*, 2020). More than 10 T_1 plants were screened by application of 0.2% Basta (Rely 280, BASF, Iselin, NJ, USA). Several single-insertion homozygous T_3 lines were established based on Basta resistance.

Transient expression in Nicotiana benthamiana

Suspensions of *A. tumefaciens* cells containing the *35S::SbCYP79A61*, *35S::ZmCYP79A61*, *35S::AtCYP79B2*, or pCC0995 (vector control) constructs were infiltrated into leaves of *N. benthamiana* as previously described (Norkunas *et al.*, 2018). Briefly, suspensions of transformed bacteria were adjusted to an OD_{600} of 0.6 in infiltration buffer (10 mM $MgCl_2$, 10 mM MES, pH 5.6), and acetosyringone was added to a final concentration of 150 μM. Bacterial suspensions were then incubated at room temperature for 1 h and loaded into a blunt-tipped plastic syringe that was used to infiltrate the underside of leaves of 3-week-old plantlets. The 3–4 fully expanded leaves of independent plantlets were infiltrated with cell suspensions containing the different vectors. After 3 d, leaf tissue samples were harvested, extracted, and analyzed for aldoxime content.

RNA extraction and quantitative reverse transcription–PCR (qRT–PCR) analysis

To measure the expression level of *SbCYP79A61* in Arabidopsis transgenic lines overexpressing *SbCYP79A61*, total RNA was isolated from 2-week-old leaves of transgenic lines and control plants by using the QIAGEN RNeasy Plant Mini Kit (QIAGEN, Germantown, MD, USA; 74904). A 5 μg aliquot of total RNA was treated with DNase following the manufacturer's protocol, and 1 μg of RNA was used for first-strand cDNA synthesis employing a reverse transcription kit (ThermoFisher Scientific, MA, USA; 4368814). qPCRs were performed in a 10 μl volume mix using SYBR Green components (ThermoFisher Scientific; A25742) in a StepOnePlus Real-time PCR system (Applied Biosystems). *SbCYP79A61* transcripts were amplified with the following primers: forward primer (5′-ACCCTCTTCGCTTCAACCC-3′) and reverse primer (5′-ATGATGCTCATAGCAGTGCCG-3′). Gene expression was normalized to the reference gene *TUB3* (At5g62700), which was amplified with the following primers: forward primer (5′-TGGTGGA GCCTTACAACGCTACTT-3′) and reverse primer (5′-TTCACAGCA AGCTTACGGAGGTCA-3′). Relative expression was calculated based on the $2^{-\Delta\Delta Ct}$ method (Livak and Schmittgen, 2001). qRT–PCR analysis was conducted with three biological replicates.

Metabolite analysis

Glucosinolates were extracted from 3-week-old Arabidopsis leaves following the method described in Perez *et al.* (2021). A 10 μl aliquot of extracts was analyzed on an UltiMate 3000 HPLC system (ThermoFisher Scientific) equipped with a diode array detector (DAD) in the UV-vis region 200–500 nm. The compounds were separated on an Acclaim™ RSLC120 C18 column (100 mm×3 mm; 2.2 μm) with a flow rate of 0.5 ml min^{-1} (ThermoFisher Scientific). Solvent A [0.1% formic acid (v/v) in water] and solvent B (acetonitrile) were used as mobile phases with a gradient program as follow: 0.3–5 min, 5–14%; 5–8.25 min, 14–14.5%; 8.25–11.5 min, 14.5–18%; and 11.5–15 min, 18–95% of solvent B increase. The column temperature was 40 °C. The contents of benzyl glucosinolate and indole glucosinolate were quantified based on the peak area at 220 nm, and the authentic standards benzyl glucosinolate (EMDMillipore Sigma, PHL89216) and indol-3-ylmethyl glucosinolate (EMDMillipore Sigma, PHL80593) were used for quantification. Soluble metabolite analyses were conducted with four biological replicates.

Feeding assay

Leaf segments (~10–12 cm) of the first leaves of 8-day-old maize and sorghum seedlings were placed in aqueous solutions containing 0.005% (v/v) Triton X-100 alone, with 30 μM of unlabeled or stable isotope, deuterium-labeled PAOx (containing deuterium atoms attached to benzyl ring carbons), or with 30 μM of labeled or unlabeled benzyl cyanide. Unlabeled benzyl cyanide and labeled benzyl cyanide (benzyl cyanide-α-^{13}C) were purchased from EMDMillipore Sigma (B19401 and 486973). Labeled and unlabeled PAOx were synthesized as described in Perez *et al.* (2021). Feeding assays were conducted with 3–4 biological replicates. After 24 h of incubation, samples were removed from the solutions, dried, weighed, flash-frozen in liquid nitrogen, and stored at −80 °C until extraction.

Aldoxime and D_5-PAA detection using LC-MS

Aldoxime synthesis, aldoxime, and D_5-PAA extraction, and D_5-PAA detection were performed using methods described in Perez *et al.* (2021). Briefly, 50–100 mg FW samples were extracted in 1 ml of cold sodium phosphate buffer (50 mM, pH 7.0) containing 0.1% (w/v) diethyl dithiocarbamic acid sodium salt and incubated at 4 °C for 1 h. After adjusting the sample pH to 2.7 with hydrochloric acid, samples were purified with HLB columns (WAT094225; Waters, MA, USA) as described in Perez *et al.* (2021). After evaporating the purified samples *in vacuo*, they were resuspended in water. LC solutions and gradient program, mass spectrometer and ionization parameters, and multiple reaction monitoring

(MRM) for D_5-PAA detection were described previously (Perez *et al.*, 2021).

For IAOx and PAOx detection, all samples were resuspended in water after extraction and analyzed using Vanquish Horizon ultra-high performance liquid chromatography (UHPLC) installed with an Eclipse Plus C18 column (2.1 × 50 mm, 1.8 µm) (Aligent), and mass analysis was performed using a TSQ Altis Triple Quadruple (Thermo Scientific) MS/MS system with an ion funnel. The mass spectrometer was operated in positive ionization mode at an ion spray voltage of 4800 V. Formic acid (0.1%) in water and 100% acetonitrile were used as mobile phases A and B, respectively, with a gradient program (0–95% mobile phase B over 4 min) at a flow rate of 0.4 ml min^{-1}. The sheath gas, aux gas, and sweep gas were set at 50, 9, and 1 (arbitrary units), respectively. Ion transfer tube and vaporizer temperatures were set at 325 °C and 350 °C, respectively. For MRM, both Q1 and Q3 resolutions were set at 0.7 full width at half maximum (FWHM) with argon at 1.5 mTorr as collision-induced dissociation gas. The scan cycle time was 0.8 s. MRM was used to monitor parent ion→product ion transitions for each analyte as follows: mass-to-charge ratio (m/z) 175.087→158 [collision energy (CE) 16 V] for IAOx and m/z 136→119 (CE 14 V) for PAOx.

Quantification of PAA and benzyl cyanide and detection of labeled PAA and benzyl cyanide using GC-MS

To quantify PAA and benzyl cyanide we used a method adapted from Schmelz *et al.* (2004). Briefly, tissues were flash-frozen in liquid nitrogen and 100 mg were extracted in 300 µl of H_2O:1-propanol:HCl (1:2:0.005) spiked with 100 ng of D_7-PAA as an internal standard. Samples were homogenized using 1 g of ceramic beads in a Fast Prep homogenizer and further extracted with 1 ml of methylene chloride. The samples were centrifuged and the methylene chloride:1-propanol layer was collected and derivatized with trimethylsilyldiazomethane, quenched with acetic acid in hexane, and volatile compounds were collected by vapor phase extraction on SuperQ columns. Volatiles were eluted in methylene chloride and analyzed using GC-MS [GC, Agilent 7890B; MS, Agilent 5977B; column, Agilent DB-35MS (length, 30 m; diameter. 0.25 mm; film thickness, 0.25 µm)] with chemical ionization using iso-butane. The ions monitored and retention times (RTs) for the compounds are as follows: derivatized PAA (methyl phenylacetate) (m/z 151, RT 6.74 min), derivatized D_7-PAA (methyl D_7-phenylacetate) (m/z 158, RT 6.71 min), derivatized PAA-α-^{13}C (methyl phenylacetate-α-^{13}C) (m/z 152, RT 6.74 min), benzyl cyanide (m/z 118, RT 6.79 min), benzyl cyanide-α-^{13}C (m/z 119, RT 6.79 min), and D_5-benzyl cyanide (m/z 123, RT 6.78 min). Compounds were confirmed and quantified using authentic standards. Volatile compound analysis was conducted with 3–4 biological replicates.

Data analysis

Statistical analyses for all experiments were conducted in R (version 4.0.2) and RStudio (version 1.3.1056). For datasets with two categories or treatments, statistical significance was determined using Student's *t*-test. For datasets with three or more categories, statistical significance was determined using ANOVA and Tukey's test.

Accession numbers

Sequence data for proteins and genes discussed in this study can be found in GenBank under the following identifiers: SbCYP79A61 (*Sobic.010G172200*, XP_002438593.1); SbCYP79A1 (*Sobic.001G012300*, XP_002466099.1); SbCYP79A89 (*Sobic.001G185900*, OQU91462.1); SbCYP79A91 (*Sobic.001G187400*, XP_002464329.1); SbCYP79A92 (*Sobic.001G187500*, XP_002464333.1); SbCYP79A93 (*Sobic.001G187600*, XP_002464334.2); SbCYP79A94 (*Sobic005G157600*, OQU83670.1); SbCYP79A95 (*Sobic.005G158200*, XP_002449720.2); SbCYP79A96 (*Sobic.007G090457*,XP_002446424.1);SbCYP71E1(*Sobic.001G012200*, XP_002466097.1); ZmCYP79A61 (*GRMZM2G138248*, AKJ87843.1); GRMZM2G011156 (*GRMZM2G011156*, XP_008644689.1); GRMZM2G105185 (*GRMZM2G105185*, XP_008665466.1); GRMZM2G178351 (*GRMZM2G178351*, XP_008644663.1); AtCYP79B2 (*At4g39950*, NP_001328605.1); AtCYP79B3 (*At2g22330*, NP_001323954.1); AtCYP79A2 (*At5g05260*, NP_001318481.1); AtCYP79F1 (*At1g16410*, NP_563996.2); AtCYP79F2 (*At1g16400*, NP_563995.2); AtCYP79C1 (*At1g79370*, NP_178055.2); AtCYP79C2 (*At1g58260*, NP_176122.2); AtCYP83A1 (*At4g13770*, NP_193113.1); AtCYP83B1 (*At4g31500*, NP_194878.1); PrCYP79D73 (*PrCYP79D73*, AZT89153.1); PtCYP79D6 (*Potri.013G157200*, AHF20912.1); PtCYP79D7 (*Potri.013G157300*, AHF20913.1); HzCYP79A8 (XP_044954760); and HzCYP79A12 (ACM24114.1).

Results

Identification of CYP79 homologs in Sorghum bicolor

CYP79 monooxygenases catalyze aldoxime formation in many plant species. The maize genome contains four genes encoding CYP79 enzymes, one of which, ZmCYP79A61, has been shown to produce IAOx and PAOx (Irmisch *et al.*, 2015). In maize, the aldoximes IAOx and PAOx act as precursors of the auxins IAA and PAA, respectively (Perez *et al.*, 2021). In sorghum, however, the only CYP79 enzyme with known function is SbCYP79A1, which produces *p*-hydroxyphenylacetaldoxime, the precursor for dhurrin, from tyrosine (Koch *et al.*, 1995; Sibbesen *et al.*, 1995; Bak *et al.*, 2000). Given the universal occurrence of auxins and the similarities in genome sequence and organization between maize and sorghum, we hypothesized that sorghum ZmCYP79A61 homologs can generate IAOx and PAOx.

To identify putative CYP79-encoding genes in sorghum, we screened the genome of *S. bicolor* v3.1.1 using the Phytozome (v12) database with the maize ZmCYP79A61 protein sequence as a query. This initial search identified nine candidate sequences that included SbCYP79A1 (*Sobic.001G012300*). According to the CYP450 nomenclature committee (Nelson, 2009), the remaining eight sequences are annotated as SbCYP79A61 (*Sobic.010G172200*), SbCYP79A89 (*Sobic.001G185900*), SbCYP79A91 (*Sobic.001G187400*), SbCYP79A92 (*Sobic.001G187500*), SbCYP79A93 (*Sobic.001G187600*), SbCYP79A94 (*Sobic005G157600*), SbCYP79A95 (*Sobic.005G158200*), and SbCYP79A96 (*Sobic.007G090457*).

Phylogenetic analysis of the sorghum and maize CYP79 enzymes was performed using these protein sequences, as well as characterized CYP79 enzymes from Arabidopsis, barley (*Hordeum vulgare*) (Knoch *et al.*, 2016), *P. rubra* (Dhandapani *et al.*, 2019), and poplar (*P. trichocarpa*) (Irmisch *et al.*, 2013). In the resulting phylogenetic tree, the maize and sorghum CYP79s were split among two major subclades (Fig. 1). One subclade includes three maize CYP79s (GRMZM2G011156,

GRMZM2G105185, and GRMZM2G178351) and seven sorghum CYP79s (SbCYP79A89, 91–96). The other subclade includes SbCYP79A61, SbCYP79A1, ZmCYP79A61, HvCYP79A12, and HvCYP79A8, and is close to CYP79s from Arabidopsis, plumeria, and poplar known to be involved in aromatic aldoxime production (Fig. 1). It was previously shown that *GRMZM2G011156*, *GRMZM2G105185*, and *GRMZM2G178351* are not expressed in most organs (Irmisch *et al.*, 2015). Similarly, the six *SbCYP79* genes in this subclade, with the exception of *SbCYP79A95*, have low or no expression in sorghum tissues (Supplementary Fig. S1) (EMBL-EBI Expression Atlas, https://www.ebi.ac.uk/gxa/experiments/E-MTAB-3839/Result). *SbCYP79A1* is highly expressed in most tissues except flowers, whereas *SbCYP79A61* is expressed in aerial tissues including flowers and shoots (Supplementary Fig. S1). The ORF of *SbCYP79A61* encodes a protein of 547 amino acids, which, when aligned with maize ZmCYP79A61, revealed 84.3% amino acid identity (Supplementary Fig. S2; Supplementary Table S1). SbCYP79A61 contains motifs conserved among other CYP79A proteins such as the heme-binding site ([S/T]F[S/T]TGRRGCxA), the FxP[E/D]RH motif, and the NP motif (Bak *et al.*, 2006) (Supplementary Fig. S2). Given the results of the expression pattern analysis and phylogenetic analysis, SbCYP79A61 is the most likely candidate for a sorghum enzyme involved in the biosynthesis of IAOx or PAOx.

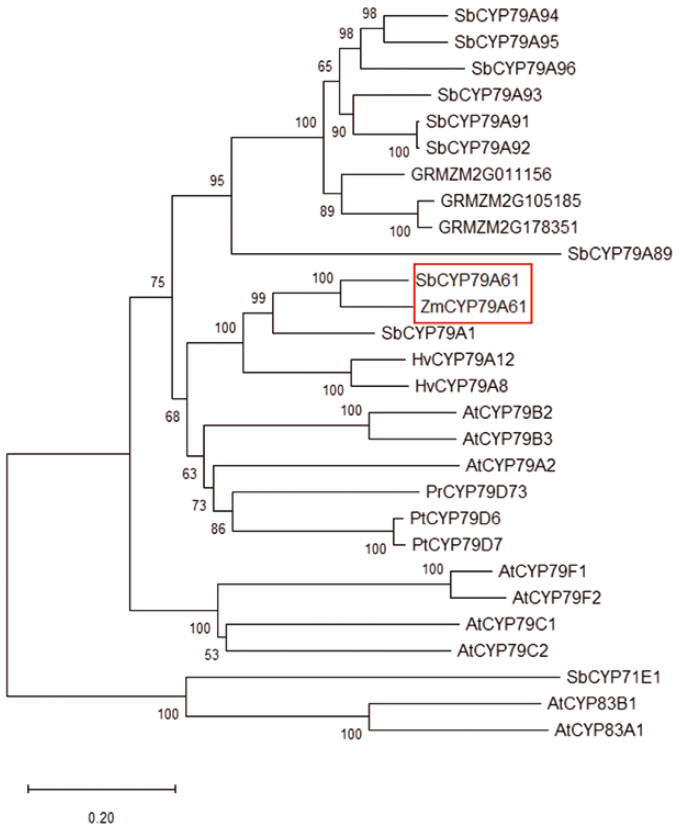

Fig. 1. Phylogenetic tree of CYP79 amino acid sequences from sorghum, maize, Arabidopsis, *Plumeria rubra*, and poplar. The red box highlights the position of the ZmCYP79A61/SbCYP79A61 subclade. The rooted tree was inferred with the Neighbor–Joining method and *n*=1000 replicates for bootstrapping. Bootstrap values are shown next to each node. As outgroups, the enzymes CYP71E1 from sorghum and CYP83A1/B1 from Arabidopsis were chosen. Accession numbers are provided in the Materials and methods.

Biochemical characterization of SbCYP79A61

To determine if SbCYP79A61 can produce PAOx or IAOx, we transiently expressed *SbCYP79A61* under the control of the *CaMV35S* promoter in *N. benthamiana* (Fig. 2). As controls for aldoxime production, *N. benthamiana* plants were infiltrated with *A. tumefaciens* harboring vectors containing *ZmCYP79A61* (for IAOx and PAOx production), *AtCYP79B2* (for IAOx production), or the vector alone as a negative control. The maize ZmCYP79A61 can act upon both tryptophan and phenylalanine, albeit with lower affinity towards tryptophan, whereas Arabidopsis AtCYP79B2 only produces IAOx (Fig. 2) (Irmisch *et al.*, 2015; Zhao *et al.*, 2002). As expected, both IAOx and PAOx were observed in leaves expressing *ZmCYP79A61* and only IAOx was observed in leaves expressing *AtCYP79B2*. Interestingly only PAOx but not IAOx was detectable in leaves expressing *SbCYP79A61* (Fig. 2), suggesting that SbCYP79A61 has activity towards phenylalanine *in vivo*.

To confirm the specificity of SbCYP79A61 for phenylalanine, we generated stable Arabidopsis transformants expressing *SbCYP79A61* (Fig. 3A) in the wild type and an IAOx-deficient mutant. The Arabidopsis ecotype used in this study, Columbia-0 (Col-0), accumulates indole glucosinolates, which are derived from IAOx, but not PAOx-derived benzyl glucosinolate in leaf tissue (Fig. 3B, C) (Kliebenstein *et al.*, 2001; Perez *et al.*, 2021). If SbCYP79A61 activity results in PAOx production, we hypothesized the Arabidopsis wild-type plants expressing *SbCYP79A61* would produce benzyl glucosinolates. The *cyp79b2 cyp79b3* double mutant (*b2b3*) is incapable of generating IAOx due to disruption of IAOx-producing enzymes CYP79B2 and CYP79B3, and, therefore, does not produce indole glucosinolates (Fig. 3C) (Zhao, 2002). If, on the other hand, SbCYP79A61 activity results in IAOx production, we hypothesized that the Arabidopsis *b2b3* mutants expressing *SbCYP79A61* would produce indole glucosinolates. Two overexpression lines in the wild-type background and two in the *b2b3* background were established and named *ox-1/WT*, *ox-2/WT*, *ox-11/b2b3*, and *ox-12/b2b3*. All *SbCYP79A61* overexpression lines were found to produce benzyl glucosinolate, while the wild type and *b2b3* mutant did not produce it (Fig. 3B). This suggests that SbCYP79A61 can produce PAOx from phenylalanine. However, indole glucosinolates in *ox-11/b2b3* and *ox-12/b2b3* were below the detection limit and were not increased in lines *ox-1/WT* and *ox-2/WT* (Fig. 3C).

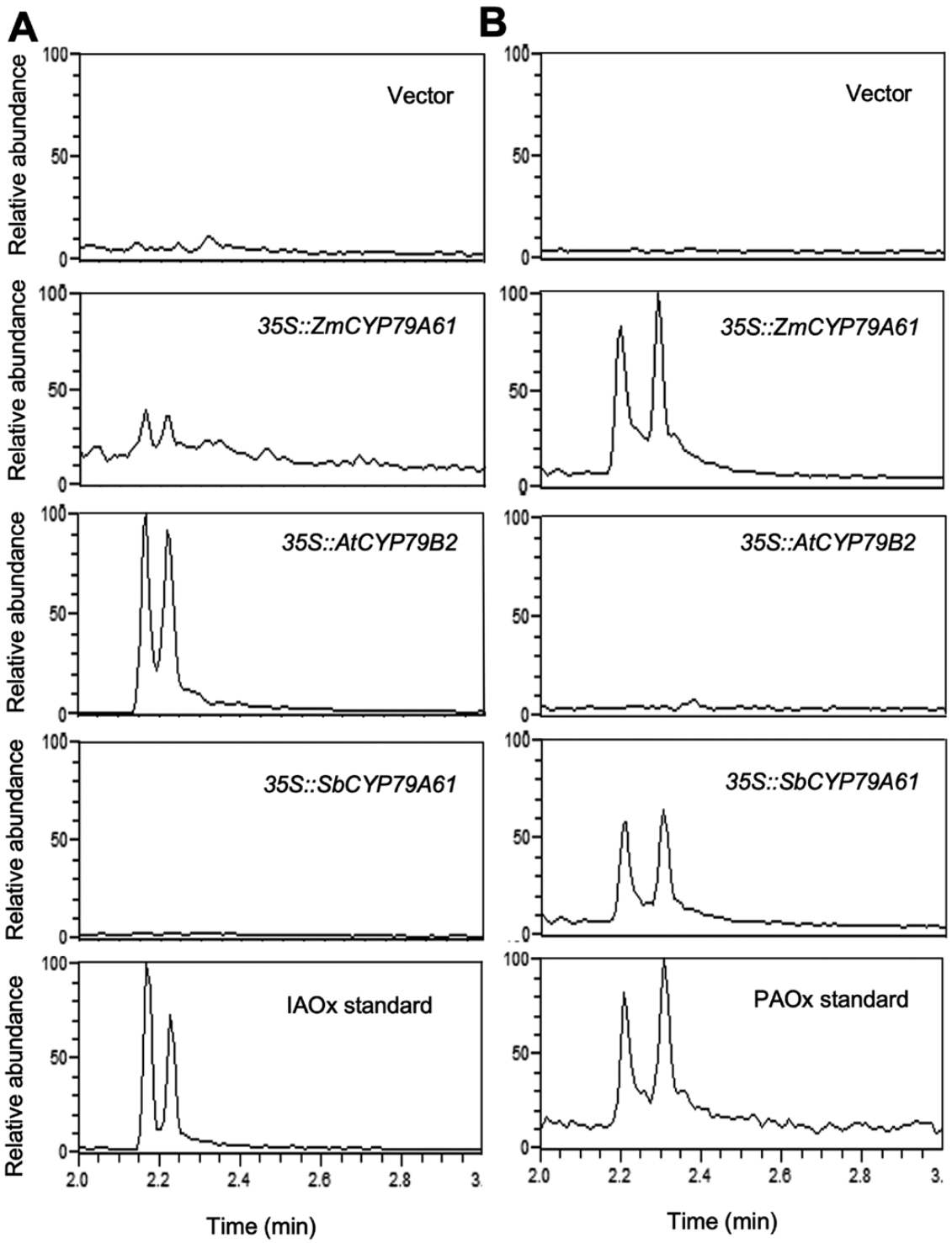

Fig. 2. Transient expression of *SbCYP79A61* in *N. benthamiana* produces PAOx. LC-MS chromatograms for IAOx (A) and PAOx (B) in *N. benthamiana* leaves of 3-week-old plantlets after infiltration with *Agrobacterium tumefaciens* strains harboring constructs containing the CYP79 genes *ZmCYP79A61* (second from top), *AtCYP79B2* (third from top), or *SbCYP79A61* (fourth from top). Chromatograms at the top represent plants infiltrated with *A. tumefaciens* harboring the empty vector, and chromatograms on the bottom display aldoxime standards. Shown are extracted ion chromatograms for IAOx (*m/z* 175.087→158) and for PAOx (*m/z* 136→119). Samples were taken 3 d after infiltration.

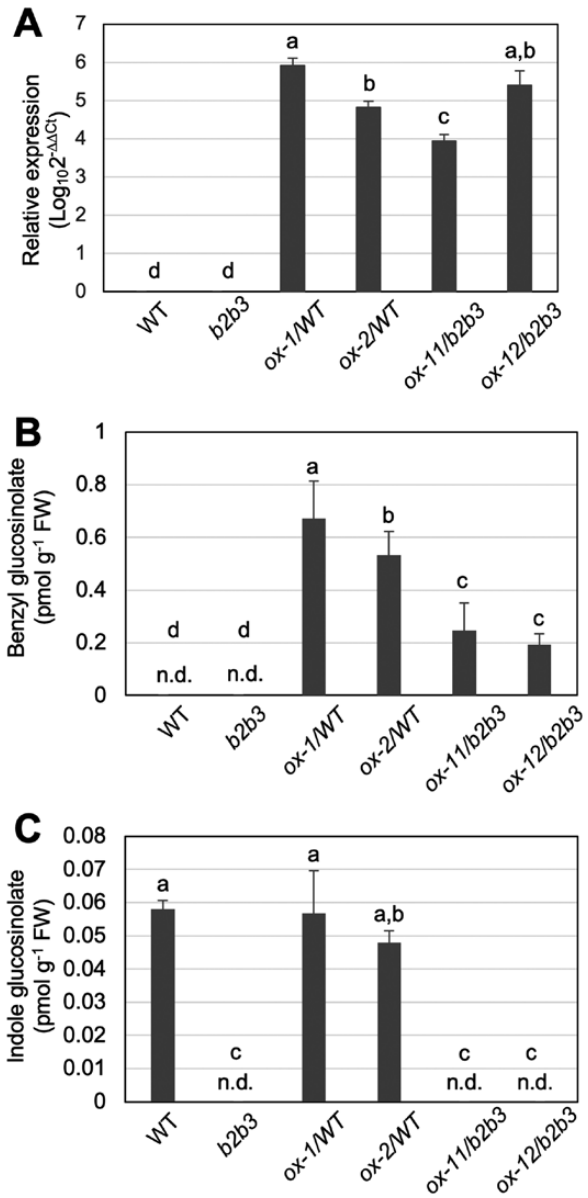

Fig. 3. Overexpression of *SbCYP79A61* in Arabidopsis results in accumulation of benzyl glucosinolate but not indole glucosinolate. (A) Relative expression ($log_{10}2^{-\Delta\Delta Ct}$) of *SbCYP79A61* in wild-type, *b2b3*, and *SbCYP79A61* overexpression lines in the wild-type (*ox-1/WT, ox-2/WT*) and *b2b3* (*ox-11/b2b3, ox-12/b2b3*) genetic backgrounds (n=3). (B) Benzyl glucosinolate concentration of wild-type, *b2b3*, and *SbCYP79A61* overexpression lines (n=4). (C) Indole glucosinolate (I3M) concentration of wild-type, *b2b3*, and *SbCYP79A61* overexpression lines (n=4). Metabolite content was analyzed from 2-week-old whole aerial parts. Bars represent the mean, and error bars represent the SD. The means were compared by one-way ANOVA, and statistically significant differences among sample means (P<0.05) were identified by Tukey's test and indicated by different lowercase letters.

These results are consistent with our *N. benthamiana* infiltration results (Fig. 2) and suggest that SbCYP79A61 has high activity towards phenylalanine, but little or no activity towards tryptophan.

Benzyl cyanide is an intermediate of the PAOx-derived PAA biosynthesis in monocots

As PAOx can act as a precursor to PAA in Arabidopsis and maize, we used feeding and isotope labeling studies to investigate the existence of this pathway in sorghum (Perez *et al.*, 2021). The feeding of sorghum leaves with PAOx led to significantly increased levels of PAA compared with water-fed samples (Fig. 4A). Additionally, when sorghum leaves were fed with D_5-PAOx, they were found to produce D_5-PAA (Fig. 4B–D) upon LC-MS analysis. On the other hand, water-fed sorghum leaves were unable to produce D_5-PAA (Fig. 4B–D). These results suggest that sorghum, like maize and Arabidopsis, can utilize PAOx generated from SbCYP79A61 to produce PAA.

As glucosinolate degradation produces nitriles such as benzyl cyanide and indole-3-acetonitrile, and nitrilases convert nitriles to acetic acid, it has been proposed that benzyl cyanide can be a precursor of PAA in Arabidopsis (Urbancsok *et al.*, 2018). Several studies have shown that PAOx serves as a precursor of benzyl cyanide as part of the volatile emission of various species (Irmisch et al., 2013, 2014, 2015; Dhandapani *et al.*, 2019). Thus, we hypothesized that benzyl cyanide might be derived from PAOx and an intermediate of the PAOx-derived PAA biosynthesis in sorghum. To test this hypothesis, we examined benzyl cyanide production in sorghum plants fed with PAOx. We detected a compound with an m/z of 118 that accumulated in PAOx-fed sorghum plants but was absent in water-fed plants. MS analysis identified this compound as benzyl cyanide (Fig. 5A), which was confirmed with an authentic standard. To determine if benzyl cyanide is directly made from PAOx in sorghum, we analyzed D_5-PAOx-fed samples for the presence of deuterium-labeled D_5-benzyl cyanide. We detected a compound with m/z 123 and retention time matching that of benzyl cyanide in sorghum upon feeding with D_5-PAOx, but not water (Fig. 5A). As D_5-benzyl cyanide has an m/z of 123, these results suggest that sorghum can directly convert PAOx to benzyl cyanide.

It was shown that nitrilase can take benzyl cyanide as a substrate in poplar, Arabidopsis, and sorghum (Jenrich *et al.*, 2007; Günther *et al.*, 2018; Urbancsok *et al.*, 2018). Thus, one possible model of PAOx-derived PAA biosynthesis would be that PAOx is converted to benzyl cyanide, which can then be acted upon by nitrilases and ultimately converted to PAA. To test this model, we analyzed PAA content after benzyl cyanide feeding in sorghum and detected increased levels of PAA (Fig. 5B). This suggests that benzyl cyanide can positively affect PAA accumulation, possibly by serving as a precursor of PAA or by activating PAA biosynthesis.

To determine if benzyl cyanide is converted to PAA, we analyzed sorghum plants after feeding with labeled benzyl cyanide-α-^{13}C. To quantify and detect PAA using GC-MS, PAA must be derivatized with trimethylsilyldiazomethane to yield the volatile compound methyl phenylacetate. This

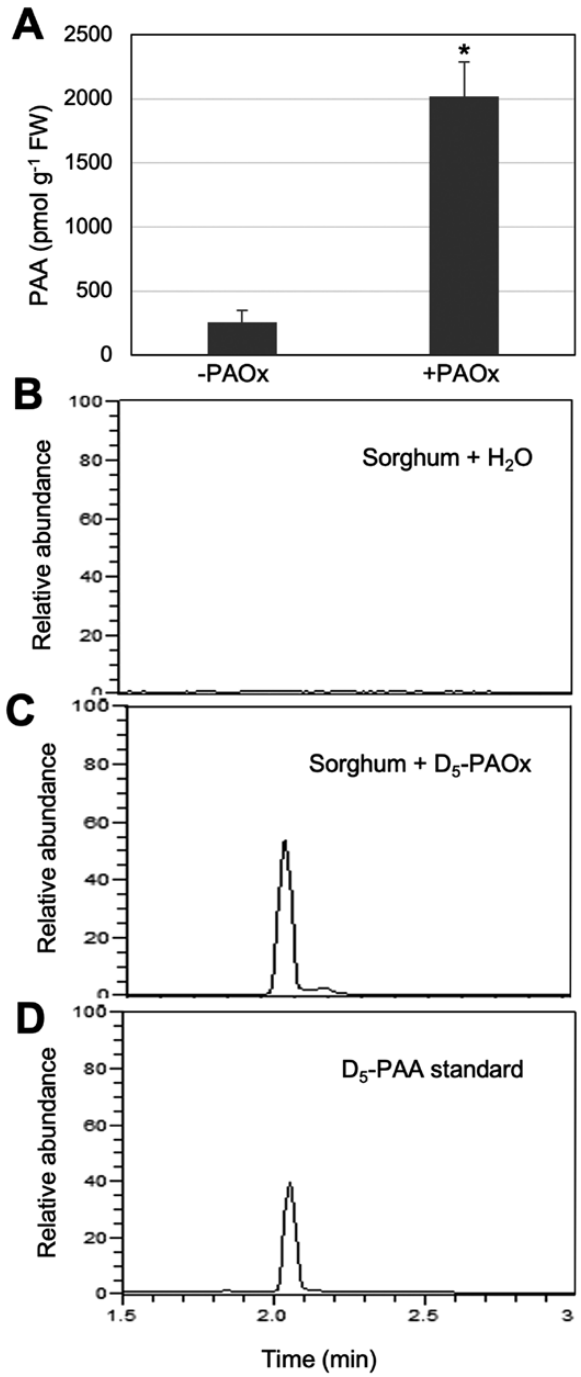

Fig. 4. Sorghum can synthesize PAA from PAOx. (A) Free PAA content of sorghum leaves fed with water or PAOx (n=3). Bars represent the mean, and error bars represent the SD. The means were compared by Student's t-test, and statistically significant differences (P<0.05) are indicated by asterisks (*). (B–D) LC-MS chromatograms for the D_5-PAA standard (D) and endogenous D_5-PAA in sorghum leaves after feeding with water (B) or D_5-PAOx (C). Shown are extracted ion chromatograms for D_5-PAA (m/z 140.077→96). Leaf segments of 8-day-old sorghum plants were incubated with either water or 30 μM of aldoximes for 24 h.

derivatization results in an increase of 14 atomic mass units. Hence, for GC-MS detection and quantification of unlabeled and labeled PAA, mass spectrometers were set to detect compounds with the adjusted m/z values. A compound with m/z 152 was detected after feeding with benzyl cyanide-α-^{13}C but not water (Fig. 5B). This m/z matched that of methyl phenylacetate-α-^{13}C, the derivatized form of PAA-α-^{13}C, which is expected if benzyl cyanide acts as a precursor of PAA, and was confirmed with the authentic standard (Sigma Cat. #293849).

To determine if these results and pathways are shared between sorghum and maize, we also performed a similar series of feeding assays in maize. As with sorghum, feeding of maize with D_5-PAOx but not water resulted in the accumulation of a compound with an m/z and retention time identical to those of D_5-benzyl cyanide (Supplementary Fig. S3A, B). Feeding with benzyl cyanide resulted in the accumulation of PAA in maize (Supplementary Fig. S3C), while feeding with benzyl cyanide-α-^{13}C but not water resulted in the detection of a metabolite with an m/z identical to that of methyl phenylacetate-α-^{13}C (Supplementary Fig. S3D, E). Taken together, these results demonstrate that benzyl cyanide is a derivative of PAOx metabolism and serves as a direct precursor of PAA in both sorghum and maize (Fig. 5C).

Discussion

Here we identified SbCYP79A61 as an enzyme capable of generating PAOx in sorghum. Despite high amino acid sequence similarity between ZmCYP79A61 and SbCYP79A61 (Supplementary Fig. S1), the two enzymes had differing substrate specificities, with SbCYP79A61 having activity towards phenylalanine but little or no activity towards tryptophan, whereas ZmCYP79A61 produces both IAOx and PAOx (Figs 2, 3). An additional point of interest with the monocot CYP79s is their clustering into two distinct clades (Fig. 1). One clade contains the aromatic-aldoxime-producing enzymes SbCYP79A1, SbCYP79A61, and ZmCYP79A61, and is part of a larger clade that contains aromatic-aldoxime-producing enzymes from dicots. The second, larger clade consists of the remaining three maize and seven sorghum CYP79 enzymes. Overall, these CYP79s, except for SbCYP79A95, have low expression compared with their characterized counterparts (Supplementary Fig. S1) (Irmisch *et al.*, 2015) and the enzymes form a clade separate from the examined CYP79s capable of producing aromatic or aliphatic aldoximes (Fig. 1), which makes prediction of their activity difficult. Given that two barley aliphatic-aldoxime-producing enzymes, HvCYP79A12 and HvCYP79A8 (Knoch *et al.*, 2016), are in the same clade with SbCYP79A1, SbCYP79A61, and ZmCYP79A61, it is possible that the remaining three maize and seven sorghum CYP79 enzymes in the second clade may not be aldoxime-producing enzymes. Further study is required to identify their catalytic activities.

Other monooxygenases that are not CYPs have been found to catalyze aldoxime production. Specifically, Thodberg *et al.* (2020) identified a fern oxime synthase (FOS1) within the species *Phlebodium aureum* and *Pteridium aquilinum* capable of catalyzing either one or two *N*-hydroxylations on phenylalanine

to generate *N*-hydroxyphenylalanine and PAOx, respectively. This study identified the first instance of a non-CYP79 enzyme catalyzing amino acid to oxime conversion and provided a mechanism by which cyanogenic ferns that do not possess CYP79 enzymes can generate cyanogenic glycosides (Harper *et al.*, 1976; Santos *et al.*, 2005). The existence of FOS1 greatly expands the number of species potentially able to generate aldoximes, and the recent discovery of a new clade of FMOs capable of catalyzing *N*-hydroxylations (Liscombe *et al.*, 2022) provides an additional target for identifying aldoxime production enzymes in both lower and higher plants, including sorghum.

While analyzing the potential role of SbCYP79A61 in sorghum, we determined that PAOx-derived PAA biosynthesis occurs in sorghum (Fig. 4) and identified benzyl cyanide as an intermediate of PAOx-derived PAA in sorghum and maize (Fig. 5; Supplementary Fig. S3). It has been proposed that nitriles such as indole-3-acetonitrile (IAN) are intermediates of aldoxime-derived auxin biosynthesis, based on the observation that Arabidopsis fed with labeled IAOx produces labeled IAN (Sugawara *et al.*, 2009). Given that nitriles such as IAN and benzyl cyanide are products of glucosinolate degradation, it was unclear if IAN or benzyl cyanide is indeed an intermediate of aldoxime-derived auxin biosynthesis bypassing glucosinolate catabolism in Arabidopsis. However, our study revealed that benzyl cyanide is directly converted from PAOx and an intermediate of the PAOx-derived PAA biosynthesis in monocots. PAA is less active but more abundant than IAA (Wightman and Rauthan, 1974; Sugawara *et al.*, 2015; Aoi *et al.*, 2020). Although both IAA and PAA are synthesized through the well-characterized YUC pathway using amino transferases (TAAs) and monooxygenases (YUCs), evidence indicates that they may be produced through distinctive biosynthesis pathways (Cook and Ross, 2016; Cook, 2019; Aoi *et al.*, 2020). For example, in the maize TAA1-deficient mutant *wei8-1*, IAA, but not PAA, is decreased substantially, suggesting an alternative route of PAA production in maize (Cook *et al.*, 2016). The PAOx-derived PAA pathway may contribute to the PAA pool in monocots. As both PAOx and benzyl cyanide production occur widely in the plant kingdom and are induced by stressors (Irmisch *et al.*, 2013; McCormick *et al.*, 2014; Luck *et al.*, 2016; Günther *et al.*, 2018; Dhandapani *et al.*, 2019; Liao *et al.*, 2020), it is likely that PAOx-derived PAA biosynthesis contributes significantly to the pool of PAA in plants under stress. CYP71 enzymes have been shown to convert aldoximes to nitriles in various species (Nafisi *et al.*, 2007; Klein *et al.*, 2013; Yamaguchi et al., 2014, 2016; Irmisch *et al.*, 2014; Liao *et al.*, 2020). In sorghum, glutathione transferases of the plant-specific lambda class (GSTLs) produce *p*-hydroxyphenyl acetonitrile as an intermediate of the dhurrin recycling process, which is further converted to *p*-hydroxyphenylacetic acid by nitrilases (Jenrich *et al.*, 2007; Bjarnholt *et al.*, 2018). Sorghum nitrilases have high activity toward *p*-hydroxyphenyl acetonitrile, but they also accept benzyl cyanide (Jenrich *et al.*, 2007). Thus, it is possible that similar enzymes may function in phenylacetaldoxime-derived phenylacetic acid production in sorghum. However, further study is needed to identify enzymes responsible for the conversion of PAOx to benzyl cyanide and to determine if IAN is an intermediate of the IAOx-derived IAA biosynthesis in plants.

We detected a significant difference in PAA and benzyl cyanide accumulation upon PAOx feeding in sorghum, with the PAA concentration increasing to ~2000 pmol g^{-1} FW (Fig. 4A), while the benzyl cyanide concentration remained relatively low at <120 pmol g^{-1} FW (Fig. 5A). On the other hand, the magnitude of PAA accumulation upon benzyl cyanide feeding in sorghum and maize was significantly different, with PAA concentration increasing >40-fold in sorghum (Fig. 5B), but only ~2.5-fold in maize (Supplementary Fig. S3C). Even though we used the same age of leaf segments for our feeding experiment, maize and sorghum develop differently, and this difference could affect the feeding efficiency. It is also possible that differences in the activities of maize and sorghum nitrilases contribute to these differences. Maize and sorghum have two and three different nitrilase enzymes, respectively (Park *et al.*, 2003; Jenrich *et al.*, 2007), and previous studies have shown that these enzymes can form heterodimers with altered substrate affinities (Jenrich *et al.*, 2007; Kriechbaumer *et al.*, 2007). Both sorghum SbNIT4A and the SbNIT4A–SbNIT4B2 heterodimer have been shown to have activity towards benzyl cyanide, with the heterodimer having a K_m value of 0.19 mM and a V_{max} of 908 nkat (mg protein)$^{-1}$ (Jenrich *et al.*, 2007). The affinity of sorghum nitrilases for benzyl cyanide is equivalent to or higher than that of the Arabidopsis nitrilases (NIT1, NIT2, and NIT3), which have K_m values ranging between 0.14 mM and 1 mM, and V_{max} values ranging from 40 pkat (mg protein)$^{-1}$ and 1400 pkat (mg protein)$^{-1}$ (Vorwerk *et al.*, 2001). Initial characterization of the maize nitrilases ZmNIT1 and ZmNIT2 demonstrated that they have activity towards IAN (Park *et al.*, 2003). Mukherjee *et al.* (2006) later showed that ZmNIT2 could hydrolyze benzyl cyanide into its corresponding acid and amide, although their experimental setup did not allow for quantification of substrate specificity. It is possible that the sorghum nitrilases have high affinity for benzyl cyanide, causing flux towards PAA to be relatively high and resulting in only low levels of benzyl cyanide accumulation and efficient conversion of benzyl cyanide to PAA in sorghum. Further research is needed to analyze the role nitrilase activity plays in PAOx-derived PAA biosynthesis.

In addition to PAA, PAOx can act as a precursor for cyanogenic glycosides. The PAOx-derived cyanogenic glycosides, amygdalin and prunasin, occur naturally in many species such as cassava, apple, and several *Prunus* species (Berenguer-Navarro *et al.*, 2002; Yamaguchi *et al.*, 2014; Bolarinwa et al., 2015, 2016; Thodberg *et al.*, 2018). Bolarinwa *et al.* (2016) reported that sorghum grains also contain amygdalin even though other studies have not corroborated this observation (Pičmanová *et al.*, 2015; Thodberg *et al.*, 2018; Jaszczak-Wilke *et al.*, 2021). We were

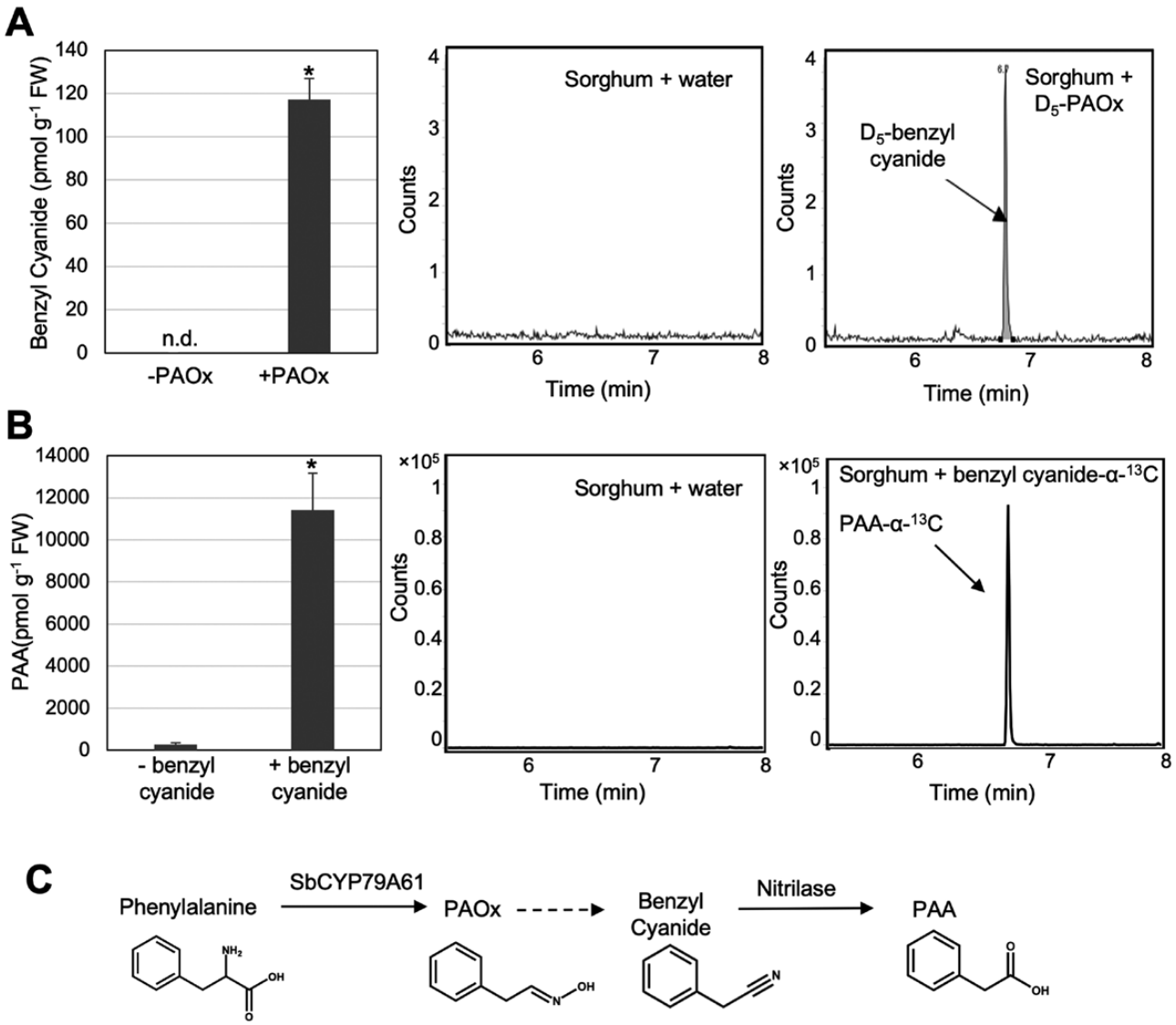

Fig. 5. Benzyl cyanide is derived from PAOx and PAA is made from benzyl cyanide in sorghum. (A) Benzyl cyanide concentration of sorghum leaves fed with water or PAOx (n=3). Bars represent the mean, and error bars represent the SD. GC-MS chromatograms set for detection of D_5-benzyl cyanide (m/z 123) in sorghum leaves fed with water or D_5-PAOx. (B) Free PAA concentration of sorghum leaves fed with water or benzyl cyanide (n=4). Bars represent the mean, and error bars represent the SD. The means were compared by Student's t-test, and statistically significant differences (P<0.05) are indicated by an asterisk (*). GC-MS chromatograms set for detection of the derivatized form of PAA-α-^{13}C, methyl phenylacetate-α-^{13}C (m/z 152), in sorghum leaves fed with water or benzyl cyanide-α-^{13}C. Leaf segments of 8-day-old sorghum plants were incubated with either water or 30 μM of aldoximes or benzyl cyanide for 24 h. The means were compared by Student's t-test, and statistically significant differences (P<0.05) are indicated by an asterisk (*). (C) Proposed model of PAOx metabolism in sorghum. In sorghum, PAOx production from phenylalanine is catalyzed by SbCYP79A61. Then, through an as yet uncharacterized reaction, PAOx is converted to benzyl cyanide. Benzyl cyanide is then in turn converted to PAA by nitrilases. This pathway of PAOx metabolism is probably shared between sorghum and maize. Note that this work and model do not exclude the possibility of additional derivates of PAOx metabolism being present in sorghum and maize, such as cyanogenic glycosides.

unable to detect amygdalin in sorghum grains of inbred lines BTx623 and RTx430 (Supplementary Fig S4). Further study is needed to identify aldoxime derivatives in sorghum.

In summary, analysis of the sorghum genome for *CYP79* homologs using phylogenetic analysis resulted in the identification of the enzyme SbCYP79A61 that catalyzes the formation of PAOx. Furthermore, data generated from feeding assays and mass spectrometric analyses of sorghum and maize plants demonstrated that sorghum is capable of PAOx-derived PAA biosynthesis, and that benzyl cyanide serves as an intermediate of this pathway in both sorghum and maize. These results suggest that PAOx and PAOx-derived metabolism may play a role in fine-tuning plant responses to various stressors.

Supplementary data

The following supplementary data are available at *JXB* online.

Table S1. List of amino acid sequence identities of SbCYP79A61 with other CYP79 enzymes.

Figure S1. Tissue-specific expression profile of *CYP79* genes in *Sorghum bicolor*.

Figure S2. Alignment of SbCYP79A61 protein sequences to maize ZmCYP79A61.

Figure S3. Production of benzyl cyanide and PAA in maize fed with PAOx.

Figure S4. Sorghum grain does not accumulate amygdalin.

Author contributions

RD, VCP, WV, AG, AKB, and JK: design of the research project; RD, VCP, AB, BT, ESAW, and JM; performing the experiments and data analysis; VCP and JK: writing. All authors read and agreed with the manuscript.

Conflict of interest

The authors have no conflicts to declare.

Funding

This work was supported by the United States Department of Agriculture (USDA)-National Institute of Food and Agriculture Hatch (005681), National Science Foundation (IOS-2142898), and a startup fund from the Horticultural Sciences Department and Institute of Food and Agricultural Sciences at the University of Florida to JK, and the United States Department of Agriculture (USDA)-Agricultural Research Service Project number 6036-11210-001-00D and the USDA-National Institute of Food and Agriculture-Specialty Crop Research Initiative grant 2018-51181-28419 to AB. National Institutes of Health (NIH)-5R35GM137893-03 to AG.

Data availability

All data supporting the findings of this study are available within the paper and within its supplementary data published online.

References

Altschul SF, Gish W, Miller W, Myers EW, Lipman DJ. 1990. Basic local alignment search tool. Journal of Molecular Biology **215**, 403–410.

Andersen MD, Busk PK, Svendsen I, Moller BL. 2000. Cytochromes P-450 from cassava (*Manihot esculenta* Crantz) catalyzing the first steps in the biosynthesis of the cyanogenic glucosides linamarin and lotaustralin: cloning, functional expression in *Pichia pastoris*, and substrate specificity of the isolated recombinant enzymes. Journal of Biological Chemistry **275**, 1966–1975.

Aoi Y, Tanaka K, Cook SD, Hayashi K-I, Kasahara H. 2020. GH3 auxin-amido synthetases alter the ratio of indole-3-acetic acid and phenylacetic acid in Arabidopsis. Plant & Cell Physiology **61**, 596–605.

Bak S, Nielsen HL, Halkier BA. 1998. The presence of CYP79 homologues in glucosinolate-producing plants shows evolutionary conservation of the enzymes in the conversion of amino acid to aldoxime in the biosynthesis of cyanogenic glucosides and glucosinolates. Plant Molecular Biology **38**, 725–734.

Bak S, Olsen CE, Halkier BA, Møller BL. 2000. Transgenic tobacco and Arabidopsis plants expressing the two multifunctional sorghum cytochrome P450 enzymes, CYP79A1 and CYP71E1, are cyanogenic and accumulate metabolites derived from intermediates in dhurrin biosynthesis. Plant Physiology **123**, 1437–1448.

Bak S, Paquette SM, Morant M, *et al*. 2006. Cyanogenic glycosides: a case study for evolution and application of cytochromes P450. Phytochemistry Reviews **5**, 309–329.

Berenguer-Navarro V, Giner-Galván RM, Grané-Teruel N, Arrazola-Paternina G. 2002. Chromatographic determination of cyanoglycosides prunasin and amygdalin in plant extracts using a porous graphitic carbon column. Journal of Agricultural and Food Chemistry **50**, 6960–6963.

Bjarnholt N, Neilson EHJ, Crocoll C, Jørgensen K, Motawia MS, Olsen CE, Dixon DP, Edwards R, Møller BL. 2018. Glutathione transferases catalyze recycling of auto-toxic cyanogenic glucosides in sorghum. The Plant Journal **94**, 1109–1125.

Blažević I, Montaut S, Burčul F, Olsen CE, Burow M, Rollin P, Agerbirk N. 2020. Glucosinolate structural diversity, identification, chemical synthesis and metabolism in plants. Phytochemistry **169**, 112100.

Bolarinwa IF, Olaniyan SA, Olatunde SJ, Ayandokun FT, Olaifa IA. 2016. Effect of processing on amygdalin and cyanide contents of some Nigerian foods. Journal of Chemical and Pharmaceutical Research **8**, 106–113.

Bolarinwa IF, Orfila C, Morgan MRA. 2015. Determination of amygdalin in apple seeds, fresh apples and processed apple juices. Food Chemistry **170**, 437–442.

Chen S, Glawischnig E, Jørgensen K, Naur P, Jørgensen B, Olsen C-E, Hansen CH, Rasmussen H, Pickett JA, Halkier BA. 2003. CYP79F1 and CYP79F2 have distinct functions in the biosynthesis of aliphatic glucosinolates in Arabidopsis. The Plant Journal **33**, 923–937.

Cook SD. 2019. An historical review of phenylacetic acid. Plant & Cell Physiology **60**, 243–254.

Cook SD, Nichols DS, Smith J, Chourey PS, McAdam EL, Quittenden L, Ross JJ. 2016. Auxin biosynthesis: are the indole-3-acetic acid and phenylacetic acid biosynthesis pathways mirror images? Plant Physiology **171**, 12.

Cook SD, Ross JJ. 2016. The auxins, IAA and PAA, are synthesized by similar steps catalyzed by different enzymes. Plant Signaling & Behavior **11**, e1250993.

Dhandapani S, Jin J, Sridhar V, Chua N-H, Jang I-C. 2019. CYP79D73 participates in biosynthesis of floral scent compound 2-phenylethanol in *Plumeria rubra*. Plant Physiology **180**, 171–184.

Edgar RC. 2004. MUSCLE: multiple sequence alignment with high accuracy and high throughput. Nucleic Acids Research **32**, 1792–1797.

Glawischnig E. 2007. Camalexin. Phytochemistry **68**, 401–406.

Glawischnig E, Hansen BG, Olsen CE, Halkier BA. 2004. Camalexin is synthesized from indole-3-acetaldoxime, a key branching point between primary and secondary metabolism in Arabidopsis. Proceedings of the National Academy of Sciences, USA **101**, 8245–8250.

Günther J, Irmisch S, Lackus ND, Reichelt M, Gershenzon J, Köllner TG. 2018. The nitrilase PtNIT1 catabolizes herbivore-induced nitriles in *Populus trichocarpa*. BMC Plant Biology **18**, 251.

Halkier BA, Gershenzon J. 2006. Biology and biochemistry of glucosinolates. Annual Review of Plant Biology **57**, 303–333.

Hansen CC, Sørensen M, Veiga TAM, Zibrandtsen JFS, Heskes AM, Olsen CE, Boughton BA, Møller BL, Neilson EHJ. 2018. Reconfigured cyanogenic glucoside biosynthesis in *Eucalyptus cladocalyx* involves a cytochrome P450. Plant Physiology **178**, 15.

Harper NL, Cooper-Driver GA, Swain T. 1976. A survey for cyanogenesis in ferns and gymnosperms. Phytochemistry **15**, 1764–1767.

Harun S, Abdullah-Zawawi M-R, Goh H-H, Mohamed-Hussein Z-A. 2020. A comprehensive gene inventory for glucosinolate biosynthetic

pathway in *Arabidopsis thaliana*. Journal of Agricultural and Food Chemistry **68**, 7281–7297.

Irmisch S, McCormick AC, Boeckler GA, *et al*. 2013. Two herbivore-induced cytochrome P450 enzymes CYP79D6 and CYP79D7 catalyze the formation of volatile aldoximes involved in poplar defense. The Plant Cell **25**, 4737–4754.

Irmisch S, McCormick AC, Günther J, Schmidt A, Boeckler GA, Gershenzon J, Unsicker SB, Köllner TG. 2014. Herbivore-induced poplar cytochrome P450 enzymes of the CYP71 family convert aldoximes to nitriles which repel a generalist caterpillar. The Plant Journal **80**, 1095–1107.

Irmisch S, Zeltner P, Handrick V, Gershenzon J, Köllner TG. 2015. The maize cytochrome P450 CYP79A61 produces phenylacetaldoxime and indole-3-acetaldoxime in heterologous systems and might contribute to plant defense and auxin formation. BMC Plant Biology **15**, 128.

Jaszczak-Wilke E, Polkowska Z, Koprowski M, Owsianik K, Mitchell AE, Bałczewski P. 2021. Amygdalin: toxicity, anticancer activity and analytical procedures for its determination in plant seeds. Molecules **26**, 2253.

Jenrich R, Trompetter I, Bak S, Olsen CE, Moller BL, Piotrowski M. 2007. Evolution of heteromeric nitrilase complexes in Poaceae with new functions in nitrile metabolism. Proceedings of the National Academy of Sciences, USA **104**, 18848–18853.

Kindl H, Schiefer S. 1971. Aldoximes as intermediates in the biosynthesis of tyrosol and tyrosol derivatives. Phytochemistry **10**, 1795–1802.

Klein AP, Anarat-Cappillino G, Sattely ES. 2013. Minimum set of cytochromes P450 for reconstituting the biosynthesis of camalexin, a major *Arabidopsis* antibiotic. Angewandte Chemie International Edition **52**, 13625–13628.

Kliebenstein DJ, Kroymann J, Brown P, Figuth A, Pedersen D, Gershenzon J, Mitchell-Olds T. 2001. Genetic control of natural variation in Arabidopsis glucosinolate accumulation. Plant Physiology **126**, 811–825.

Knoch E, Motawie MS, Olsen CE, Møller BL, Lyngkjær MF. 2016. Biosynthesis of the leucine derived α-, β- and γ-hydroxynitrile glucosides in barley (*Hordeum vulgare* L.). The Plant Journal **88**, 247–256.

Koch BM, Sibbesen O, Halkier BA, Svendsen I, Møller BL. 1995. The primary sequence of cytochrome P450tyr, the multifunctional N-hydroxylase catalyzing the conversion of L-tyrosine to p-hydroxyphenylacetaldehyde oxime in the biosynthesis of the cyanogenic glucoside dhurrin in *Sorghum bicolor* (L.) Moench. Archives of Biochemistry and Biophysics **323**, 177–186.

Kriechbaumer V, Park WJ, Piotrowski M, Meeley RB, Gierl A, Glawischnig E. 2007. Maize nitrilases have a dual role in auxin homeostasis and β-cyanoalanine hydrolysis. Journal of Experimental Botany **58**, 4225–4233.

Kumar S, Stecher G, Li M, Knyaz C, Tamura K. 2018. MEGA X: Molecular Evolutionary Genetics Analysis across computing platforms. Molecular Biology and Evolution **35**, 1547–1549.

Lai D, Maimann AB, Macea E, *et al*. 2020. Biosynthesis of cyanogenic glucosides in *Phaseolus lunatus* and the evolution of oxime-based defenses. Plant Direct **4**, e00244.

Liao Y, Zeng L, Tan H, Cheng S, Dong F, Yang Z. 2020. biochemical pathway of benzyl nitrile derived from L-phenylalanine in tea (*Camellia sinensis*) and its formation in response to postharvest stresses. Journal of Agricultural and Food Chemistry **68**, 1397–1404.

Liscombe DK, Kamiyoshihara Y, Ghironzi. 2022. A flavin-dependent monooxygenase produces nitrogenous tomato aroma volatiles using cysteine as a nitrogen source. Proceedings of the National Academy of Sciences, USA **119**, e2118676119.

Livak KJ, Schmittgen TD. 2001. Analysis of relative gene expression data using real-time quantitative PCR and the $2^{-\Delta\Delta CT}$ method. Methods **25**, 402–408.

Luck K, Jia Q, Huber M, Handrick V, Wong GK-S, Nelson DR, Chen F, Gershenzon J, Köllner TG. 2017. CYP79 P450 monooxygenases in gymnosperms: CYP79A118 is associated with the formation of taxiphyllin in *Taxus baccata*. Plant Molecular Biology **95**, 169–180.

Luck K, Jirschitzka J, Irmisch S, Huber M, Gershenzon J, Köllner TG. 2016. CYP79D enzymes contribute to jasmonic acid-induced formation of aldoximes and other nitrogenous volatiles in two *Erythroxylum* species. BMC Plant Biology **16**, 215.

McCormick AC, Irmisch S, Reinecke A, Boeckler GA, Veit D, Reichelt M, Hansson BS, Gershenzon J, Köllner TG, Unsicker SB. 2014. Herbivore-induced volatile emission in black poplar: regulation and role in attracting herbivore enemies. Plant, Cell & Environment **37**, 1909–1923.

Mikkelsen MD, Hansen CH, Wittstock U, Halkier BA. 2000. Cytochrome P450 CYP79B2 from *Arabidopsis* catalyzes the conversion of tryptophan to indole-3-acetaldoxime, a precursor of indole glucosinolates and indole-3-acetic acid. Journal of Biological Chemistry **275**, 33712–33717.

Mukherjee C, Zhu D, Biehl ER, Parmar RR, Hua L. 2006. Enzymatic nitrile hydrolysis catalyzed by nitrilase ZmNIT2 from maize: an unprecedented β-hydroxy functionality enhanced amide formation. Tetrahedron **62**, 6150–6154.

Nafisi M, Goregaoker S, Botanga CJ, Glawischnig E, Olsen CE, Halkier BA, Glazebrook J. 2007. *Arabidopsis* cytochrome P450 monooxygenase 71A13 catalyzes the conversion of indole-3-acetaldoxime in camalexin synthesis. The Plant Cell **19**, 2039–2052.

Nelson DR. 2009. The cytochrome P450 homepage. Human Genomics **4**, 59.

Nielsen JS, Møller BL. 1999. Biosynthesis of cyanogenic glucosides in *Triglochin maritima* and the involvement of cytochrome P450 enzymes. Archives of Biochemistry and Biophysics **368**, 121–130.

Nielsen JS, Møller BL. 2000. Cloning and expression of cytochrome P450 enzymes catalyzing the conversion of tyrosine to *p* -hydroxyphenylacetaldoxime in the biosynthesis of cyanogenic glucosides in *Triglochin maritima*. Plant Physiology **122**, 1311–1322.

Norkunas K, Harding R, Dale J, Dugdale B. 2018. Improving agroinfiltration-based transient gene expression in *Nicotiana benthamiana*. Plant Methods **14**, 71.

Park WJ, Kriechbaumer V, Müller A, Piotrowski M, Meeley RB, Gierl A, Glawischnig E. 2003. The nitrilase ZmNIT2 converts indole-3-acetonitrile to indole-3-acetic acid. Plant Physiology **133**, 794–802.

Paterson AH, Bowers JE, Bruggmann R, *et al*. 2009. The *Sorghum bicolor* genome and the diversification of grasses. Nature **457**, 551–556.

Perez VC, Dai R, Bai B, *et al*. 2021. Aldoximes are precursors of auxins in Arabidopsis and maize. New Phytologist **231**, 1449–1461.

Pičmanová M, Neilson EH, Motawia MS, *et al*. 2015. A recycling pathway for cyanogenic glycosides evidenced by the comparative metabolic profiling in three cyanogenic plant species. The Biochemical Journal **469**, 375–389.

Santos MG, Kelecom A, de Paiva SR, de Moraes MG, Rocha L, Garrett R. 2005. Phytochemical studies in pteridophytes growing in Brazil: a review. The Americas Journal of Plant Science and Biotechnology **14**, 113–125.

Schmelz EA, Engelberth J, Tumlinson JH, Block A, Alborn HT. 2004. The use of vapor phase extraction in metabolic profiling of phytohormones and other metabolites. The Plant Journal **39**, 790–808.

Schnable PS, Ware D, Fulton RS, *et al*. 2009. The B73 maize genome: complexity, diversity, and dynamics. Science **326**, 1112–1115.

Sibbesen O, Kock B, Halkier BA, Møller BL. 1995. Cytochrome P-450TYR is a multifunctional heme-thiolate enzyme catalyzing the conversion of L-tyrosine to p-hydroxyphenylacetaldehyde oxime in the biosynthesis of the cyanogenic glucoside dhurrin in *Sorghum bicolor* (L.) Moench. Journal of Biological Chemistry **270**, 3506–3511.

Sørensen M, Neilson EHJ, Møller BL. 2018. Oximes: unrecognized chameleons in general and specialized plant metabolism. Molecular Plant **11**, 95–117.

Sugawara S, Hishiyama S, Jikumaru Y, Hanada A, Nishimura T, Koshiba T, Zhao Y, Kamiya Y, Kasahara H. 2009. Biochemical analyses of indole-3-acetaldoxime-dependent auxin biosynthesis in Arabidopsis. Proceedings of the National Academy of Sciences, USA **106**, 5430–5435.

Sugawara S, Mashiguchi K, Tanaka K, *et al*. 2015. Distinct characteristics of indole-3-acetic acid and phenylacetic acid, two common auxins in plants. Plant & Cell Physiology **56**, 1641–1654.

Tapper BA, Conn EE, Butler GW. 1967. Conversion of α-keto-isovaleric acid oxime and isobutyraldoxime to linamarin in flax seedlings. Archives of Biochemistry and Biophysics **119**, 593–595.

Thodberg S, Del Cueto J, Mazzeo R, Pavan S, Lotti C, Dicenta F, Jakobsen Neilson EH, Møller BL, Sánchez-Pérez R. 2018. Elucidation of the amygdalin pathway reveals the metabolic basis of bitter and sweet almonds (*Prunus dulcis*). Plant Physiology **178**, 1096–1111.

Thodberg S, Sørensen M, Bellucci M, Crocoll C, Bendtsen AK, Nelson DR, Motawia MS, Møller BL, Neilson EHJ. 2020. A flavin-dependent monooxygenase catalyzes the initial step in cyanogenic glycoside synthesis in ferns. Communications Biology **3**, 507.

Underhill EW. 1967. Biosynthesis of mustard oil glucosides: conversion of phenylacetaldehyde oxime and 3-phenylpropionaldehyde oxime to glucotropaeolin and gluconasturtiin. European Journal of Biochemistry **2**, 61–63.

Urbancsok J, Bones AM, Kissen R. 2018. Benzyl cyanide leads to auxin-like effects through the action of nitrilases in *Arabidopsis thaliana*. Frontiers in Plant Science **9**, 1240.

Vorwerk S, Biernacki S, Hillebrand H, Janzik I, Müller A, Weiler EW, Piotrowski M. 2001. Enzymatic characterization of the recombinant *Arabidopsis thaliana* nitrilase subfamily encoded by the NIT 2/ NIT 1/NIT 3-gene cluster. Planta **212**, 508–516.

Wang C, Dissing MM, Agerbirk N, Crocoll C, Halkier BA. 2020. Characterization of Arabidopsis CYP79C1 and CYP79C2 by glucosinolate pathway engineering in *Nicotiana benthamiana* shows substrate specificity toward a range of aliphatic and aromatic amino acids. Frontiers in Plant Science **11**, 57.

Weng J-K, Mo H, Chapple C. 2010. Over-expression of F5H in COMT-deficient Arabidopsis leads to enrichment of an unusual lignin and disruption of pollen wall formation: lignin modification leads to male sterility. The Plant Journal **64**, 898–911.

Wightman F, Rauthan BS. 1974. Evidence for the biosynthesis and natural occurrence of the auxin, phenylacetic acid, in shoots of higher plants. In: Plant Growth Substances; 8th International Conference of Plant Growth Substances. 15–27.

Wittstock U, Halkier BA. 2000. Cytochrome P450 CYP79A2 from *Arabidopsis thaliana* L. catalyzes the conversion of L-phenylalanine to phenylacetaldoxime in the biosynthesis of benzylglucosinolate. Journal of Biological Chemistry **275**, 14659–14666.

Yamaguchi T, Matsui Y, Kitaoka N, Kuwahara Y, Asano Y, Matsuura H, Sunohara Y, Matsumoto H. 2021. A promiscuous fatty acid ω-hydroxylase CYP94A90 is likely to be involved in biosynthesis of a floral nitro compound in loquat (*Eriobotrya japonica*). New Phytologist **231**, 1157–1170.

Yamaguchi T, Noge K, Asano Y. 2016. Cytochrome P450 CYP71AT96 catalyses the final step of herbivore-induced phenylacetonitrile biosynthesis in the giant knotweed, *Fallopia sachalinensis*. Plant Molecular Biology **91**, 229–239.

Yamaguchi T, Yamamoto K, Asano Y. 2014. Identification and characterization of CYP79D16 and CYP71AN24 catalyzing the first and second steps in l-phenylalanine-derived cyanogenic glycoside biosynthesis in the Japanese apricot, *Prunus mume* Sieb. et Zucc. Plant Molecular Biology **86**, 215–223.

Zhang D, Song YH, Dai R, Lee TG, Kim J. 2020. Aldoxime metabolism is linked to phenylpropanoid production in *Camelina sativa*. Frontiers in Plant Science **11**, 17.